



Inverse problem with beamforming regularization matrix applied to sound source localization in closed wind-tunnel using microphone array



Thomas Padois*, Philippe-Aubert Gauthier, Alain Berry

Groupe d'Acoustique de l'Université de Sherbrooke (GAUS), 2500 Boulevard de l'Université, Sherbrooke, QC, Canada J1K 2R1

ARTICLE INFO

Article history:

Received 18 December 2013

Received in revised form

21 May 2014

Accepted 23 July 2014

Handling Editor: P. Joseph

Available online 2 September 2014

ABSTRACT

Microphone arrays have become a standard technique to localize and quantify source in aerodynamics. The simplest approach is the beamforming that provides noise source maps with large main lobe and strong side lobes at low frequency. Since a decade, the focus is set on deconvolution techniques such as DAMAS or Clean-SC. While the source map is clearly improved, these methods require a large computation time. In this paper, we propose a sound source localization technique based on an inverse problem with beamforming regularization matrix called Hybrid Method. With synthetic data, we show that the side lobes are removed and the main lobe is narrower. Moreover, if the sound noise source map provided by this method is used as input in the DAMAS process, the number of DAMAS iterations is highly reduced. The Hybrid Method is applied to experimental data obtained in a closed wind-tunnel. In both cases of acoustic or aerodynamic data, the source is correctly detected. The proposed Hybrid Method is found simple to implement and the computation time is low if the number of scan points is reasonable.

© 2014 Elsevier Ltd. All rights reserved.

1. Introduction

Over the last two decades, phased-microphone arrays have become a standard technique to localize aeroacoustic sources [1,2]. Beamforming is a basic approach that consists in delaying and summing microphone signals. The advantage of beamforming is its simplicity and robustness. One of the main problems in beamforming is the poor spatial resolution at low frequency which somehow limits the interpretation and relevance of source maps.

To overcome this issue, techniques have been developed in the past years. One of them is a deconvolution technique called DAMAS [3] (that has been extended to DAMAS2 [4] and DAMAS-C [5]). The aim of DAMAS is to extract a source distribution from a beamforming source map by iteratively deconvolving the map. The width of the main lobe is clearly reduced with this technique and side lobes are suppressed. However, the computational cost is high and uncorrelated monopoles have to be used as the reference solutions. An alternative approach, called Clean-SC [6], has been developed. The aim is to suppress side lobes correlated with the main source. Therefore, Clean-SC cannot discriminate coherent sources. Recently, an algorithm has been developed by Suzuki [7]. After decomposing the microphone Cross Spectral Matrix (CSM) into eigenmodes, an inverse problem is defined and solved iteratively. The spatial resolution of this approach is increased

* Corresponding author.

E-mail address: thomas.padois@usherbrooke.ca (T. Padois).

but the computation time is large due to the iterative nature of the method. New methods based on sparsity constraint [8] or Bayesian approach [9] allow super-resolution in acoustic imaging, but the computation time is very large and these methods use dedicated toolbox to solve the inverse problem.

In this paper we propose an algorithm, called Hybrid Method, initially developed for sound field extrapolation [10], based on an inverse problem with beamforming regularization matrix. The idea of this regularization is to more strongly penalize the non-signal region in the inverse problem. Moreover, there is no assumption on the nature of the sources (correlated or uncorrelated) and the computation time is low if few scan points are required. The aim of this study is to compare the noise source maps provided by the inverse problem regularized with beamforming matrix and other high-resolution source identification algorithms such as Clean-SC and DAMAS. In Section 2, the Hybrid Method is introduced. The performances of the source identification algorithms are compared with synthetic data in Section 3. Section 4 is devoted to the experimental tests and results collected in a closed wind-tunnel for various types of sources.

2. Theory

2.1. Direct problem

We consider S acoustic monopole sources at location \mathbf{x}_s and M microphones at location \mathbf{x}_m . The acoustic pressure recorded by the microphones is denoted $\hat{\mathbf{p}}(\mathbf{x}_m)$ and can be written in matrix form as

$$\hat{\mathbf{p}}(\mathbf{x}_m) = \mathbf{G}(\mathbf{x}_m, \mathbf{x}_s)\mathbf{q}(\mathbf{x}_s), \quad (1)$$

where $\mathbf{G}(\mathbf{x}_m, \mathbf{x}_s) = (1/4\pi \|\mathbf{x}_m - \mathbf{x}_s\|) \exp(-jk\|\mathbf{x}_m - \mathbf{x}_s\|)$ is the free-field Green function representing the acoustic radiation between the sources and the microphones, $\mathbf{q}(\mathbf{x}_s)$ is the strength of the sources and k is the acoustic wavenumber. Bold characters are vectors or matrices and the sizes are $\mathbf{p}(\mathbf{x}_m) \in \mathbb{C}^{M \times 1}$, $\mathbf{G}(\mathbf{x}_m, \mathbf{x}_s) \in \mathbb{C}^{M \times S}$ and $\mathbf{q}(\mathbf{x}_s) \in \mathbb{C}^{S \times 1}$.

2.2. Inverse problem formulation

Basically, the aim of inverse methods is to estimate the strength of the source \mathbf{q} that creates the acoustic pressure $\hat{\mathbf{p}}$ onto the microphone array, knowing the free-field Green function \mathbf{G} . One way to define the acoustical inverse problem is to solve a minimization problem that can be written in the general form

$$\mathbf{q}_\lambda = \operatorname{argmin}\{\|\hat{\mathbf{p}} - \mathbf{G}\mathbf{q}\|_2^2 + \lambda^2 \mathcal{Q}(\mathbf{q})^2\}, \quad (2)$$

with $\mathcal{Q}(\cdot)$ a discrete smoothing norm [11] and λ a regularization parameter. The argument of the minimization problem is a Hermitian quadratic function of \mathbf{q} . The vector 2-norm is denoted by $\|\cdot\|_2$

In a similar manner, we introduce a modified version of the Eq. (2) with data scaling by a scalar β

$$\mathbf{q}_{\lambda\beta} = \operatorname{argmin}\{\|\beta\hat{\mathbf{p}} - \mathbf{G}\mathbf{q}\|_2^2 + \lambda^2 \mathcal{Q}(\mathbf{q})^2\}. \quad (3)$$

In Eq. (3), the primary goal of beta β is to compensate for reduced overall source amplitudes caused by over-regularization. This type of scalar compensation was also introduced by Moorhouse [12] with a different approach. The selection of the smoothing norm \mathcal{Q} , the regularization parameter λ and the scaling parameter β are explained in the following sections.

2.3. Inverse problem solution

It is well known that the minimization problem without regularization is ill-conditioned [13–15], meaning that the solution can be very sensitive to measurement noise or model uncertainties, therefore a discrete smoothing norm is used to regularize the unknown solution $\mathbf{q}_{\lambda\beta}$. We can define the discrete smoothing norm as

$$\mathcal{Q}(\mathbf{q}) = \|\mathbf{L}\mathbf{q}\|_2, \quad (4)$$

where \mathbf{L} is a square regularization matrix. The optimal solution of this minimization problem is obtained by setting the derivative with respect to \mathbf{q} of the cost function equation (3) to zero [16,17]

$$\mathbf{q}_{\lambda\beta} = (\mathbf{G}^H \mathbf{G} + \lambda^2 \mathbf{L}^H \mathbf{L})^{-1} \mathbf{G}^H \beta \hat{\mathbf{p}}, \quad (5)$$

where $(\cdot)^H$ is the Hermitian transpose. The solution of the minimization problem can be rewritten as

$$\mathbf{q}_{\lambda\beta} = \mathbf{L}^{-1} ([\mathbf{L}^{-1}]^T \mathbf{G}^H \mathbf{G} \mathbf{L}^{-1} + \lambda^2 \mathbf{I})^{-1} [\mathbf{L}^{-1}]^T \mathbf{G}^H \beta \hat{\mathbf{p}}, \quad (6)$$

where $(\cdot)^T$ denotes matrix transposition. Therefore the general form inverse problem $\mathbf{q}_{\lambda\beta}$ can be related to the standard form inverse problem $\underline{\mathbf{q}}_{\lambda\beta}$ thanks to the regularization matrix

$$\mathbf{q}_{\lambda\beta} = \mathbf{L}^{-1} \underline{\mathbf{q}}_{\lambda\beta} = \mathbf{L}^{-1} (\underline{\mathbf{G}}^H \underline{\mathbf{G}} + \lambda^2 \underline{\mathbf{I}})^{-1} \underline{\mathbf{G}}^H \beta \hat{\mathbf{p}}, \quad (7)$$

with $\underline{\mathbf{G}} = \mathbf{G} \mathbf{L}^{-1}$. The standard form inverse problem solution $\underline{\mathbf{q}}_{\lambda\beta}$ can be seen as a regularized inverse problem solution whereas the general form inverse problem $\mathbf{q}_{\lambda\beta}$ is regularized and scaled.

2.4. Inverse problem: classical Tikhonov regularization matrix

Basically, in the classical Tikhonov regularization the discrete smoothing norm is replaced by the identity matrix $\mathbf{L}=\mathbf{I}$ and the scaling parameter is set to $\beta=1$. Therefore, the general form solution of the inverse problem with the Tikhonov regularization can be written as

$$\mathbf{q}_\lambda = (\mathbf{G}^H \mathbf{G} + \lambda^2 \mathbf{I})^{-1} \mathbf{G}^H \hat{\mathbf{p}}, \quad (8)$$

The main difficulty of the Tikhonov regularization is the selection of the regularization parameter λ in order to get the best compromise between a small residual norm and a small solution norm. Several approaches have been proposed to select the regularization parameter based on singular value decomposition [18], condition number [16], Picard condition [19] and L-curve [11].

2.5. Inverse problem: beamforming regularization matrix

The classical Tikhonov regularization adds uniform signals to the Green function product ($\mathbf{G}^H \mathbf{G}$) in Eq. (8), but no information about the acoustic data is added. One way to perform a better regularization is to take into account the result obtained by focused beamforming. The main idea is to use a discrete smoothing norm depending on the beamforming results, giving *a priori* information about the acoustic data, instead of the identity matrix which blindly penalizes all sources.

The aim of beamforming is to delay and sum all microphone signals in relation to a virtual source position. When the source position is equal to the real source position, the sum of microphone signals is maximum. The beamforming response denoted \mathbf{q}_{BF} can be written as

$$\mathbf{q}_{\text{BF}} = \mathbf{W}^H \hat{\mathbf{p}}, \quad (9)$$

where $\mathbf{W} \in \mathbb{C}^{M \times S}$ stands for the weight matrix [6] and is expressed as

$$W_{ms} = G_{ms} / \mathbf{g}_s^H \mathbf{g}_s \quad (10)$$

where \mathbf{g}_s is the s -th column of \mathbf{G} .

The new discrete smoothing norm in relation to the beamforming, called beamforming regularization matrix [10], can be defined by

$$\mathbf{L}^{-1} = \left[\text{diag} \left(\frac{|\mathbf{W}^H \hat{\mathbf{p}}|}{\|\mathbf{W}^H \hat{\mathbf{p}}\|_\infty} \right) \right], \quad (11)$$

where $|\cdot|$ denotes elementwise absolute value of the argument and $\|\cdot\|_\infty$ is the infinite norm. The term $\text{diag}(\mathbf{A})$ means that the $[S \times 1]$ vector \mathbf{A} is mapped on the main diagonal of a $[S \times S]$ matrix. The discrete smoothing norm is normalized by the infinity norm of the beamforming to ensure that the regularization is normalized in terms of beamforming output. Therefore the maximum value of the smoothing norm \mathbf{L}^{-1} is set to 1 and corresponds to the peak value of the beamforming output.

2.6. Inverse problem: cross spectral formulation

The aim of this section is to reformulate the solution and the regularized inverse problem in terms of the Cross Spectral Matrix (CSM). Therefore, some of the quantities defined in the previous sections are redefined here. Classically, the beamforming output is expressed in terms of CSM of the sound pressure signals $\hat{\mathbf{p}}$. Therefore the CSM is introduced in the following. The beamforming output denoted \mathbf{Q}_{BF} is given by

$$\mathbf{Q}_{\text{BF}} = \mathbf{q}_{\text{BF}} \mathbf{q}_{\text{BF}}^H = \mathbf{W}^H \mathbf{C} \mathbf{W}. \quad (12)$$

The matrix \mathbf{C} is the CSM defined by $\mathbf{C} = \hat{\mathbf{p}} \hat{\mathbf{p}}^H$. Since the discrete smoothing norm equation (11) depends on the microphone sound pressures, the next step is to reformulate it in terms of CSM of microphone sound pressures. The term $|\mathbf{W}^H \hat{\mathbf{p}}|$ in Eq. (11) is a column vector formed by the absolute values of $\mathbf{W}^H \hat{\mathbf{p}}$ components. The s -th component of $|\mathbf{W}^H \hat{\mathbf{p}}|$ is

$$|\sum_m \mathbf{W}_{ms}^H \hat{\mathbf{p}}_m| = \sqrt{|\sum_m \mathbf{W}_{ms}^H \hat{\mathbf{p}}_m|^2} = \sqrt{\sum_{m,n} \mathbf{W}_{ms}^H \hat{\mathbf{p}}_m \hat{\mathbf{p}}_n^H \mathbf{W}_{ns}} = \sqrt{\text{Diag}(\mathbf{Q}_{\text{BF}})}. \quad (13)$$

Therefore $|\mathbf{W}^H \hat{\mathbf{p}}|$ is formed by the square root of the components of $\text{Diag}(\mathbf{Q}_{\text{BF}})$ where Diag is the vector formed by the main diagonal of the matrix. Similarly, $\|\mathbf{W}^H \hat{\mathbf{p}}\|_\infty$ in Eq. (11) is the maximum value of $|\mathbf{W}^H \hat{\mathbf{p}}|$ over all possible values of s and can be expressed as

$$\|\mathbf{W}^H \hat{\mathbf{p}}\|_\infty = \sqrt{\|\text{Diag}(\mathbf{Q}_{\text{BF}})\|_\infty}. \quad (14)$$

Therefore, the beamforming regularization matrix can be expressed in terms of the CSM of the sound pressure signals

$$\mathbf{L}^{-1} = \left[\text{diag} \left(\frac{\sqrt{\text{Diag}(\mathbf{Q}_{BF})}}{\sqrt{\|\text{Diag}(\mathbf{Q}_{BF})\|_\infty}} \right) \right]. \quad (15)$$

Finally, according to Eq. (7) the source power $\mathbf{Q}_{\lambda\beta} = \mathbf{q}_{\lambda\beta}\mathbf{q}_{\lambda\beta}^H$ of the general-form and the standard-form $\underline{\mathbf{Q}}_{\lambda\beta}$ inverse problems are given by

$$\mathbf{Q}_{\lambda\beta} = \mathbf{L}^{-1} \underline{\mathbf{Q}}_{\lambda\beta} (\mathbf{L}^{-1})^H = \mathbf{L}^{-1} \beta (\mathbf{J}_\lambda \underline{\mathbf{G}}^H) \mathbf{C} (\underline{\mathbf{G}} \mathbf{J}_\lambda^H) \beta^H (\mathbf{L}^{-1})^H, \quad (16)$$

with

$$\mathbf{J}_\lambda = (\underline{\mathbf{G}}^H \underline{\mathbf{G}} + \lambda^2 \mathbf{I})^{-1}. \quad (17)$$

As the beamforming regularization matrix \mathbf{L}^{-1} is expressed in terms of the beamforming weight vector \mathbf{W} , the regularized steering vector (free-field Green function) is now redefined as $\underline{\mathbf{G}} = \mathbf{W} \mathbf{L}^{-1}$. In the following for brevity sake, Eq. (16) is called Hybrid Method.

One can notice that the expression of the Hybrid Method is similar to the beamforming (i.e. a CSM multiply by weighting matrices). Therefore deconvolution algorithms based on beamforming, such as DAMAS or Clean-SC, can be implemented using the Hybrid Method at the initial result. Moreover, it could be possible to iterate the Hybrid Method by defining a new regularization matrix based on the result of the Hybrid Method at the previous step.

2.7. Inverse problem: selection of scaling parameter β

The beamforming regularization matrix Eq. (11) is used to give an *a priori* information in the regularization process and therefore to improve the noise source map. In order to fully compare the source localization algorithms, it is desirable to provide a noise source map, where the peak value indicates the source level, like in beamforming. However with the Hybrid Method and inverse problem with Tikhonov regularization, the source level depends on the selection of the regularization parameter λ . The scaling parameter β is used to compensate the discrepancy in the source peak level due to the matrix inversion brought by \mathbf{J}_λ in Eq. (16) and needs to be adjusted to satisfy the above requirements. Moorhouse proposed a method to compensate the source strength discrepancy in the case of truncated singular value decomposition or Tikhonov regularization [12]. The aim was to multiply the reconstructed sound pressure, from the inverse problem, by a scalar in order to get the same reconstructed and measured sound pressure. However, this method is more suitable in the case of low background noise which is generally not the case in a closed wind-tunnel.

If the Hybrid Method equation (16) is compared with the beamforming solution equation (12), we can notice that two terms are included, the regularization matrix \mathbf{L}^{-1} and the matrix $\mathbf{J}_\lambda = (\underline{\mathbf{G}}^H \underline{\mathbf{G}} + \lambda^2 \mathbf{I})^{-1}$. The regularization matrix \mathbf{L}^{-1} is bounded between 0 and 1, therefore it does not modify the peak value of the noise source map. The matrix $(\underline{\mathbf{G}}^H \underline{\mathbf{G}} + \lambda^2 \mathbf{I})^{-1}$ involves a modification in the source level depending on λ . If we make the assumption that the inverse problem is over-regularized, i.e. $\|\underline{\mathbf{G}}^H \underline{\mathbf{G}}\|_2 \ll \|\lambda^2 \mathbf{I}\|_2$, the 2-norm of $(\underline{\mathbf{G}}^H \underline{\mathbf{G}} + \lambda^2 \mathbf{I})^{-1}$ is approximately equal to $1/\lambda^2$ according to matrix properties. Therefore the matrix inversion introduces a division by $1/\lambda^2$ on the left hand side of \mathbf{C} in Eq. (16). To compensate this discrepancy, we use the 2-norm of $(\underline{\mathbf{G}}^H \underline{\mathbf{G}} + \lambda^2 \mathbf{I})$ which is equal to (λ^2) in the over-regularized case. Therefore, we choose to define the scaling parameter β as

$$\beta = \|\underline{\mathbf{G}}^H \underline{\mathbf{G}} + \lambda^2 \mathbf{I}\|_2. \quad (18)$$

The regularization parameter λ leading to a correct estimation of the source level is investigated in Section 3.3. Fig. 1 summarizes the different steps of the Hybrid Method.

2.8. Clean-SC

Clean-SC is one of the most commonly employed deconvolution techniques in aeroacoustics. Clean-SC removes side lobes and spots spatially coherent with the main lobe [6] obtained by beamforming. Moreover the size of the main lobe is clearly reduced as compared to beamforming. The iterative process of Clean-SC is briefly introduced here, for more information the reader can refer to [6]. In the initial step, the delay-and-sum beamforming noise source map is computed, then the peak value is searched. A new CSM due to the source distribution coherent with the peak value is constructed. The new CSM is subtracted to the initial one and the process is repeated iteratively. At the end, the peak values are replaced by monopolar point sources and added to the residual noise source map. In this paper the noise source maps given by Clean-SC are compared with the beamforming and the Hybrid Method results.

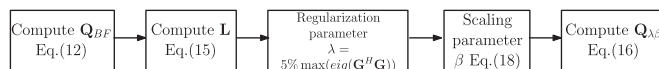


Fig. 1. Steps of the Hybrid Method algorithm.

2.9. DAMAS

Several deconvolution algorithms have been described in the literature. The Deconvolution Approach for the Mapping of Acoustic Sources (DAMAS) is one of the most efficient, but the computation time is very large. Here, we choose to use the result of the Hybrid Method at the initial step of the DAMAS process. For the sake of conciseness, the DAMAS algorithm is briefly presented. For more information, the reader should refer to [3]. The aim of the DAMAS algorithm is to solve the inverse problem $\hat{\mathbf{A}}\hat{\mathbf{X}} = \hat{\mathbf{Y}}$ where $\hat{\mathbf{A}}$ and $\hat{\mathbf{X}}$ stand for the propagation matrix and noise source level, respectively, at each grid point. The matrix $\hat{\mathbf{Y}}$ is equal to the beamforming map \mathbf{Q}_{BF} . This inverse problem is solved iteratively. The map obtained is clearly improved as compared to beamforming, with increased resolution and no side lobes.

3. Numerical application of the sound source localization methods

3.1. Problem configuration

In this section, the noise source maps obtained with the microphone array technique previously presented are compared. The aim is to highlight the abilities in terms of localization and source level quantification of the Hybrid Method. We consider the coordinate system shown in Fig. 2. A 48 spiral-arm microphone array is used, the center of the spiral is the origin (the array geometry corresponds to the experimental geometry discussed in Section 4). This geometry is commonly used in aeroacoustic source identification to provide a narrow main lobe with low side lobes [2]. The positions are made dimensionless with the source wavelength λ_s and the sound velocity c_0 is set to $c_0 = 1$. To generate acoustic waves, we consider a monopole source located at $(x_s=0, y_s=0$ and $z_s=5$). The monopole radiation is expressed in the frequency domain. The amplitude is set to $a_{mono} = 1$, \mathbf{r} is the distance vector between the source and the microphones

$$\hat{\mathbf{p}}_{mono} = \frac{a_{mono}}{4\pi \|\mathbf{r}\|} \exp(-jk\|\mathbf{r}\|). \quad (19)$$

The scan zone where the sources are searched is a square with side lengths equal to 5 located in a plane parallel to the antenna and containing the source. The scan zone is sampled with (41×41) points. Beamforming is performed without diagonal removing of \mathbf{C} . The selection of the regularization parameter λ is discussed in Section 3.3. The loop factor of Clean-SC is set to 1 [6]. DAMAS is performed over 1000 iterations and either beamforming noise source maps or Hybrid Method noise source maps are used as inputs to DAMAS.

3.2. Noise source maps

The noise source maps generated by the different microphone array techniques are presented in Fig. 3. In each case, the peak value is located at the source position and the source level is correctly estimated. Beamforming exhibits the worst map, as expected, with a large main lobe and several side lobes. Clean-SC and the Hybrid Method clearly improve the spatial resolution by narrowing the main lobe. However the best resolution is given by DAMAS but the computational time is dramatically increased as compared to Clean-SC and the Hybrid Method. To compare the DAMAS performance with the beamforming or Hybrid Method, the Root Mean Square (RMS) of the entire noise source map is computed at each iteration in Fig. 3f. DAMAS with beamforming is not converged after 500 iterations whereas DAMAS with the Hybrid Method converges after only 12 iterations. This can be explained by the initial noise source map given by the Hybrid Method which is cleaner than the beamforming noise source map. To conclude, the Hybrid Method applied to simulated data enhances the resolution similar to Clean-SC, decreases the number of iteration of DAMAS, and consequently the computation time, and estimates correctly the source level. The computation time is 20 s with the Hybrid Method, 5 s with Clean-SC and less than 1 s with beamforming on a standard PC in this case. If the number of scan points is reduced, for instance (21×21) ,

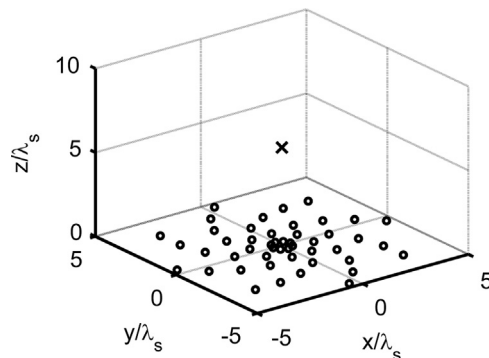


Fig. 2. Illustration of the array geometry and the coordinate system. The black dots and the cross are the microphone positions and the source position respectively.

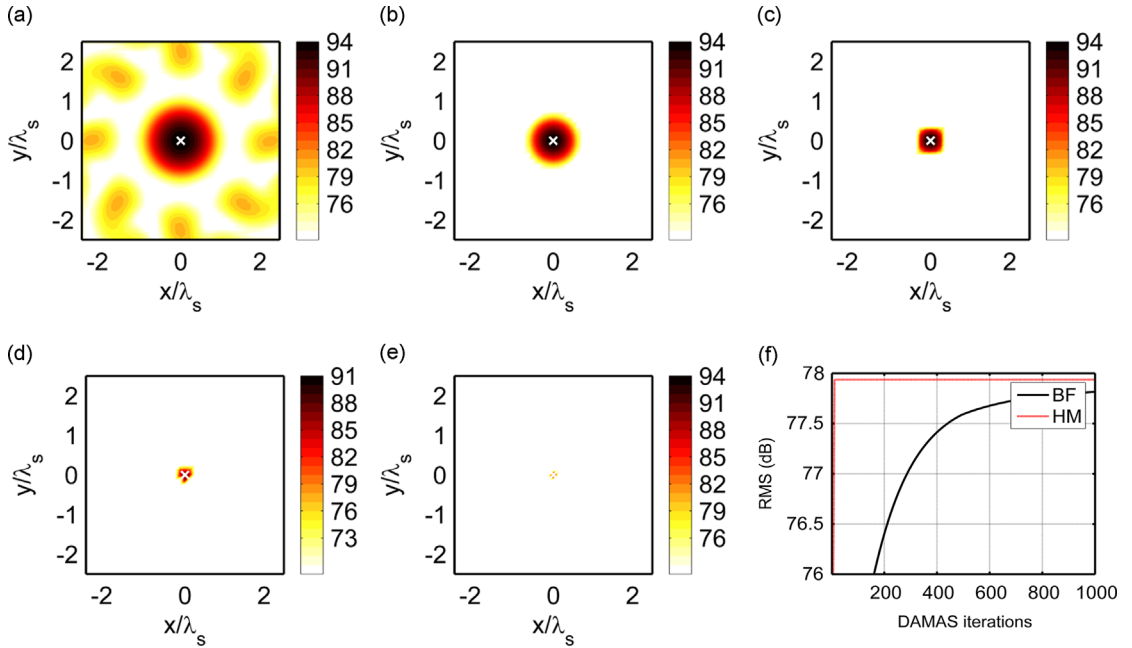


Fig. 3. Noise source maps of a simulated monopolar sound source. (a) Beamforming, (b) Hybrid Method, (c) Clean-SC, (d) DAMAS (BF) after 100 iterations, (e) DAMAS (HM) after 100 iterations and (f) Root Mean Square of the noise source maps versus the number of DAMAS iterations. The white cross represents the source position. The source level is in dB and one color level represents 1 dB. (For interpretation of the references to color in this figure caption, the reader is referred to the web version of this article.)

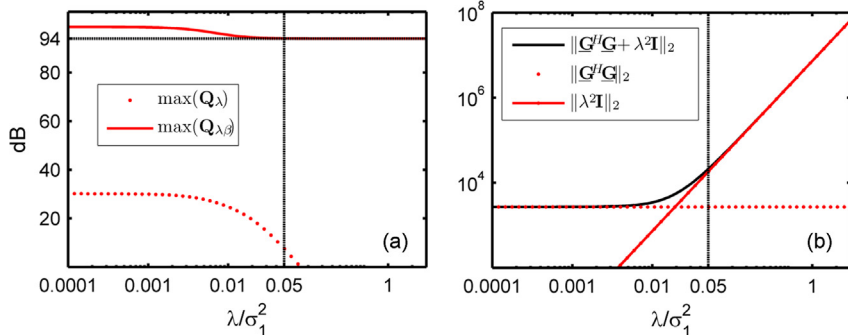


Fig. 4. (a) Evolution of the peak of the noise source map of the Hybrid Method with $\beta=1$ (\mathbf{Q}_λ) and β according to Eq. (18) ($\mathbf{Q}_{\lambda\beta}$) and (b) 2-norm of each term of the scaling parameter in Eq. (18) in relation to the parameter λ/σ_1^2 . The vertical and horizontal black lines correspond to $\lambda/\sigma_1^2 = 0.05$ and to the exact source pressure level (94 dB).

the computation time is 0.5 s with the Hybrid Method and 0.4 s with Clean-SC. The increase of the computation time of the Hybrid Method is due to the inversion of Eq. (17). With DAMAS the computation time is due to the calculation of the Point Spread Function (PSF) and the iteration process to solve the inverse problem. The computation time increases with the fourth power of the number of scan points for the PSF and with the second power for the iteration process. With the Hybrid Method the calculation of the PSF is not changed but the number of iterations is clearly decreased. DAMAS with beamforming takes 123 s to converge whereas DAMAS with the Hybrid Method takes 21 s (with (41×41) scan points).

3.3. Influence of the regularization and scaling parameters

In the previous section, the regularization parameter λ was set to $0.05\sigma_1^2$ where σ_1 is the largest eigenvalue of the matrix product $(\mathbf{G}^H\mathbf{G})$ [7]. In this case, the source level estimated by the Hybrid Method is correct. In order to illustrate the influence of the parameters λ and β , the peak value of the noise source map given by the Hybrid Method is calculated for a range of regularization parameters from $\lambda/\sigma_1^2 = 10^{-4}$ to $\lambda/\sigma_1^2 = 1$ with $\beta=1$ (\mathbf{Q}_λ) and with β the scaling parameter according to Eq. (18) ($\mathbf{Q}_{\lambda\beta}$). The evolution of the peak value of the noise source map and the 2-norm of each term of the scaling parameter in Eq. (18) are plotted in relation to the parameter λ/σ_1^2 (Fig. 4). With $\beta=1$, the source level estimated from the peak value is

never correct and it becomes very small for large values of the regularization parameter. When the scaling parameter β is introduced, we can observe two areas below and above $\lambda = 0.05\sigma_1^2$. When $\lambda/\sigma_1^2 < 0.05$, the source level is over-estimated due to the negligible effect of the regularization in the 2-norm of $(\underline{\mathbf{G}}^H \underline{\mathbf{G}} + \lambda^2 \mathbf{I})$. When $\|\underline{\mathbf{G}}^H \underline{\mathbf{G}}\|_2$ is small compared to $\|\lambda^2 \mathbf{I}\|_2$, the source level becomes correct. Therefore in the case of scaled data, the regularization parameter has to be at least 5 percent of the largest eigenvalue σ_1^2 to get the correct source level. In the following, this value is set as default.

4. Experimental application of the sound source localization methods

4.1. Laboratory experiments: set-up

An experiment has been carried out in the closed wind-tunnel of the Université de Sherbrooke to perform source localization. The test section is 10 m long and the flow is generated by a 1.8 m diameter vane axial fan driven by a 200 hp electric motor. The rotational speed of the fan, and consequently the flow velocity in the test section, can be varied using a frequency control. The air velocity in the empty 1.82 m × 1.82 m test section is approximately 25 m/s. The level of turbulence is less than 0.3 percent. The wooden, smooth walls of the test section create a reverberant environment. The closed wind-tunnel does not include any acoustic treatment, therefore a large background noise is observed, especially at multiples of the passage frequency of the fan.

The microphone array is installed on the top wall of the test section. The microphone array consists in 48 microphones with 8-arm-spiral and 6 microphones per arm (Fig. 5b). The microphones are Brüel&Kjaer phased microphones model no. 4957 and the signals are acquired with 4 LAN-XI modules. The acoustic signals are sampled at 32,768 Hz during 10 s.

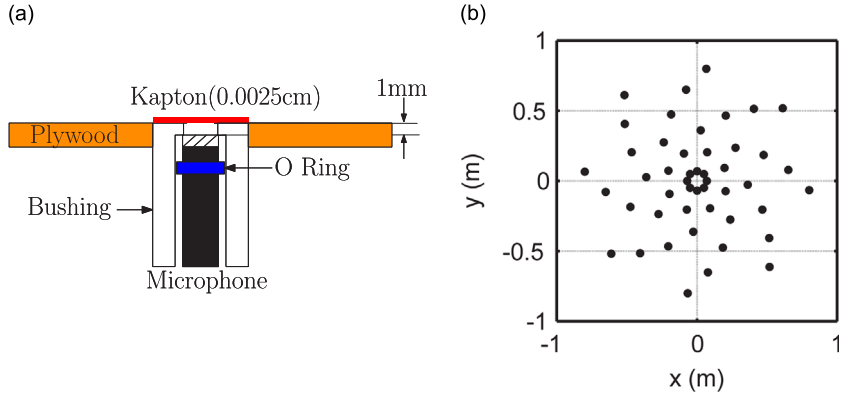


Fig. 5. Schematic of (a) a recessed microphone and (b) microphone array geometry.

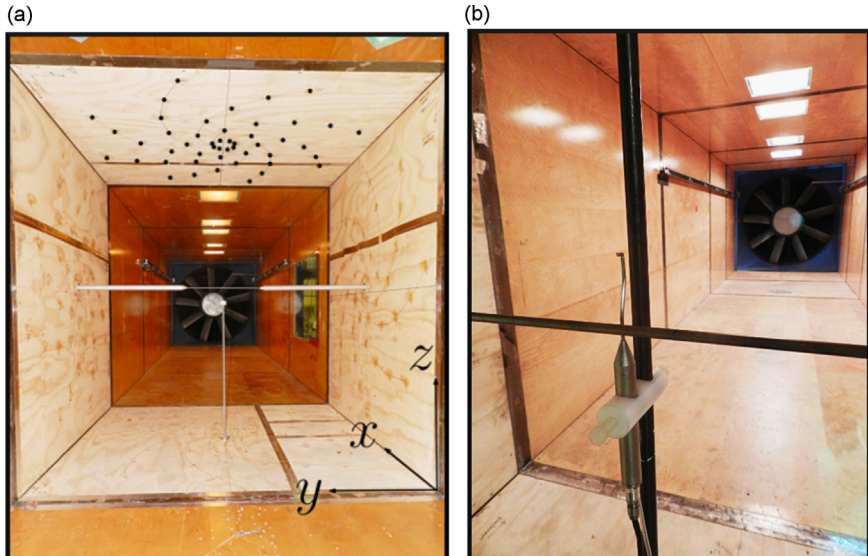


Fig. 6. (a) Picture of the cross test section of the closed wind-tunnel. (b) Close view of the Cobra Probe for aerodynamic measurements.

The test section with the microphone array is shown in Fig. 6a. The microphones are flush-mounted in a bushing slotted in the plywood top wall (Fig. 5a). The airtightness is ensured with silicone between the plywood and the bushing and with o-rings between the bushing and the microphones. The microphones are recessed in cylindrical apertures as proposed in [20] and openings in the wind-tunnel side walls are covered by a film of Kapton to protect from the hydrodynamic fluctuations. Kapton is a very thin film (0.0025 cm) similar to Kevlar.

Two types of sources are used to generate acoustic waves. The first one is a LMS Mid High Frequency Volume source that behaves as a monopolar volume acceleration source. The spherical wave spreading (6 dB reduction per distance doubling) and the constant directivity of the volume velocity source have been experimentally verified in an anechoic room in preliminary experiments [21]. The source termination is placed in the center of the cross test section using a rod installed in the floor panel. The second source is a cylinder immersed in the flow. The noise generated by the vortex shedding behind a cylinder is a pure-tone and radiates like a dipole in the direction perpendicular to the flow and cylinder axis [22,23]. Moreover the vortex shedding frequency is related to the acoustic frequency. The cylinder diameter is 6.35 mm (1/4 in) and the length is 0.45 m (see Fig. 6a). The cylinder is fixed to the right and left side walls using two rods (diameter 5 cm), therefore the vortex shedding frequency is 8 times lower than the cylinder frequency. In this case, it corresponds to approximately 100 Hz, which is below the investigated frequency range. Aerodynamic measurements have been carried out to characterize the flow. A Cobra probe able to resolve the three components of velocity was used. The time signal was sampled at 2500 Hz during 10 s. Therefore, the vortex shedding frequency could be determined. A picture of the Cobra Probe is presented in Fig. 6b.

4.2. Localization of the controlled acoustic source without flow

As a preliminary step, we used the controlled acoustic source in the absence of flow in order to validate the source identification algorithms and estimate the installation effects on the source identification results (hard-wall reflections for example). The origin of the domain is set at the bottom right of the cross test section (see Fig. 6a). The source is located at ($x_s=0.96$ m; $y_s=0.92$ m; $z_s=0.90$ m), which almost corresponds to the center of the test section.

The acoustic source was driven by a sine-wave at 1 kHz, which almost corresponds to the vortex shedding frequency determined by flow measurements. The acoustic signal was sampled at 32,768 Hz during 10 s. The CSM was computed with samples of 4096 points weighted by a Hanning window and 50 percent overlap. The scan zone is a square, parallel to the microphone array and including the source, located at 0.90 m from the array with dimensions 1.2 m \times 1.2 m. The scan zone is sampled with 41 points in each direction (total number of 1681 scan points).

The noise source maps are presented in Fig. 7 for various source identification algorithms. The beamforming noise source map exhibits a large main lobe and strong side lobes but the source position is well detected, even in the presence of hard wall reflexions. Note that in Fig. 7 the scan zone is substantially smaller than the wind tunnel section, therefore image

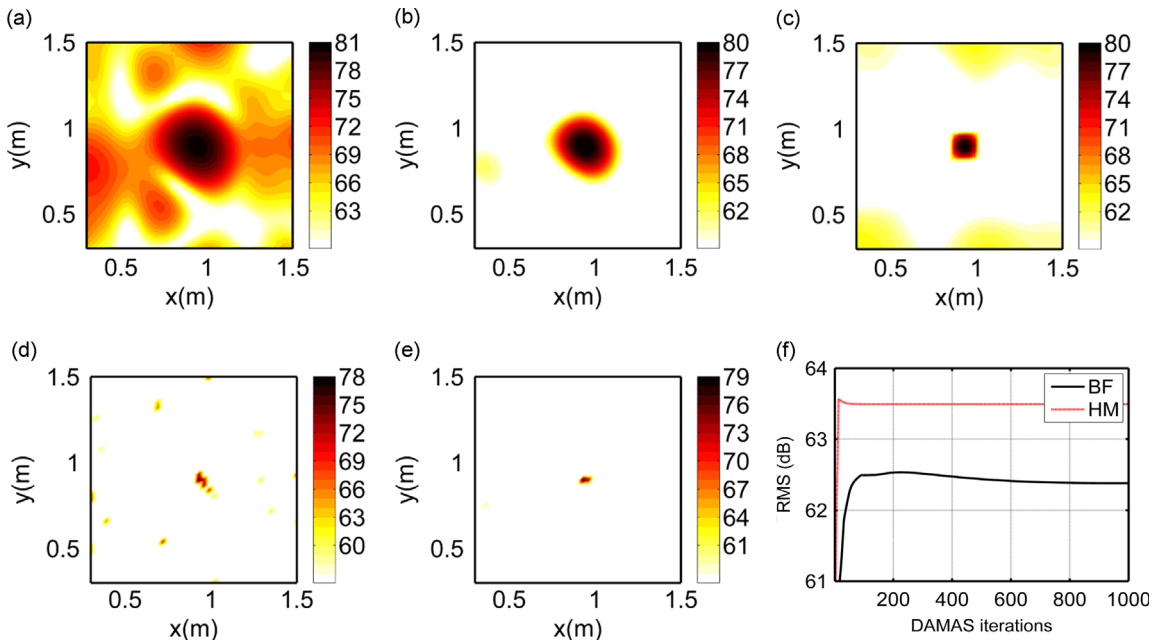


Fig. 7. Noise source maps with the controlled acoustic source driven by a sine-wave at 1 kHz (without flow). (a) Beamforming, (b) Hybrid Method, (c) Clean-SC, (d) DAMAS (BF) after 100 iterations, (e) DAMAS (HM) after 100 iterations and (f) Root Mean Square of the noise source maps versus the number of DAMAS iterations. The source level is in dB and one color level represents 1 dB. (For interpretation of the references to color in this figure caption, the reader is referred to the web version of this article.)

sources due to wall reflections cannot be detected. The Hybrid Method and Clean-SC clearly improve the noise source maps by eliminating side lobes and increasing the spatial resolution. The sound level estimated by the Hybrid Method is equivalent to the beamforming and Clean-SC results. These results are in good agreement with the simulations presented in Section 3.

Then, the Hybrid Method was used as an input in the DAMAS processing. Fig. 7d and e corresponds to the DAMAS noise source maps after 100 iterations when the initial map is the beamforming result or the Hybrid Method result. DAMAS initiated by beamforming (Fig. 7d) exhibits several spots at the source location and lower spots (full convergence was not reached) whereas DAMAS initiated by the Hybrid Method (Fig. 7e) shows only a single spot at the source position. The RMS of the noise source maps versus the number of iterations is plotted in Fig. 7f. As expected from the noise source map, DAMAS with beamforming does not converge after 500 iterations while 25 iterations are sufficient for DAMAS with the Hybrid Method. Therefore, the Hybrid Method improves the noise source map and at the same time reduces the number of DAMAS iterations.

4.3. Localization of the controlled acoustic source with flow

In this section, we study the potential of the source identification algorithms to localize a controlled sound source in a flow. The closed wind-tunnel has not been designed to perform acoustic measurements and no acoustic treatment is used. Therefore, the background noise especially at the Blade Passage Frequency (BPF=139 Hz) of the fan and its harmonics is large. The flow velocity is set to $U_0 = 23$ m/s, which corresponds to the maximum velocity of the wind-tunnel. The diameter of the rod which holds the acoustic monopole has been chosen to create a vortex shedding frequency lower than the frequency of the monopole, in order to separate the two sources in the frequency domain. On the other hand, it is known that the acoustic propagation from the controlled source is modified by the flow. The acoustic waves are convected by the mean flow and refracted by the shear or boundary layers. Here, only the convection effect is taken into account and the refraction effect due to the boundary layer is neglected. The free-field Green function is replaced by the convected Green function in order to correct for the mean convection [24]

$$\mathbf{G}(\mathbf{x}_m, \mathbf{x}_s) = \frac{1}{4\pi \|\mathbf{r}\|} \exp(-j\omega \Delta t), \quad (20)$$

with

$$\Delta t = \frac{-U_0(x_s - x_m)}{(U_0^2 - c_0^2)} + \sqrt{\frac{-(x_s - x_m)^2 + (y_s - y_m)^2 + (z_s - z_m)^2}{(U_0^2 - c_0^2)}} + \frac{U_0^2(x_s - x_m)^2}{(U_0^2 - c_0^2)^2}, \quad (21)$$

where (x_s, y_s, z_s) and (x_m, y_m, z_m) designate source and microphone positions, respectively. The beamforming noise source map is presented in Fig. 8a. The source position is correctly detected with a large spot at the source position. Strong spurious

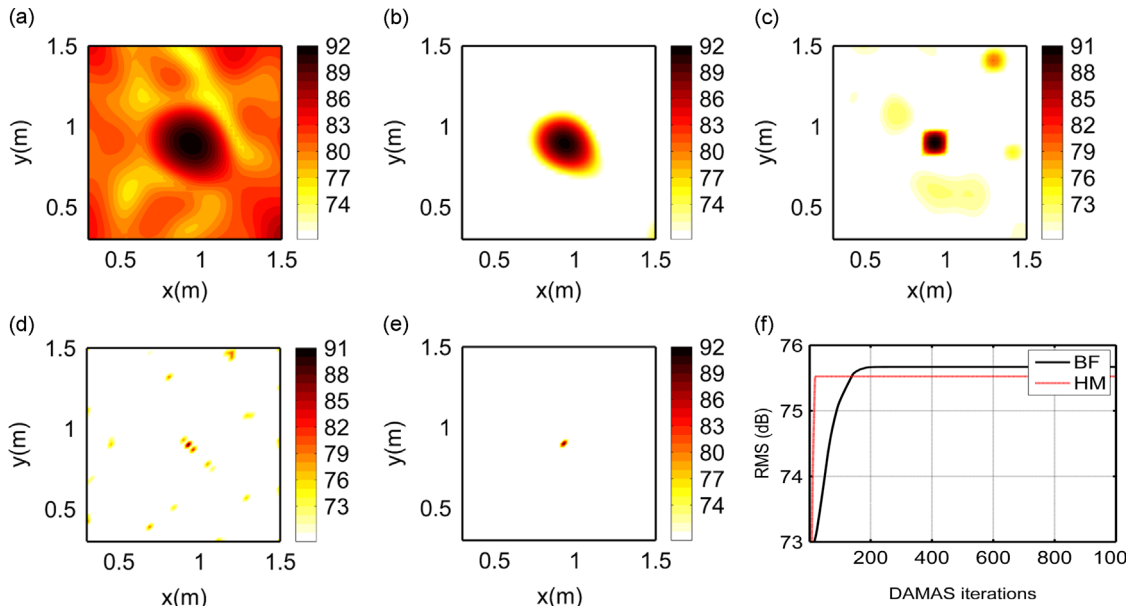


Fig. 8. Noise source maps with the controlled acoustic source driven by a sine-wave at 1 kHz (with flow $U_0 = 23$ m/s). (a) Beamforming, (b) Hybrid Method, (c) Clean-SC, (d) DAMAS (BF) after 100 iterations, (e) DAMAS (HM) after 100 iterations and (f) Root Mean Square of the noise source maps versus the number of DAMAS iterations. The source level is in dB and one color level represents 1 dB. (For interpretation of the references to color in this figure caption, the reader is referred to the web version of this article.)

lobes surround the main lobe due to high background noise in the closed wind-tunnel. However, the beamforming associated to the convected Green function is able to detect the actual source position. Fig. 8b and c shows the noise source maps obtained with the Hybrid Method and Clean-SC. The Hybrid Method exhibits a main lobe at the source position whereas Clean-SC shows also one lower source (more than 12 dB below the main source). We assume that this false source is due to the residual noise source map (last iteration of Clean-SC process). However, both methods clearly improve the noise source maps as compared to beamforming. Fig. 8d-f shows respectively the DAMAS noise source map initiated by the beamforming, initiated by the Hybrid Method and the RMS of the noise source maps versus the number of iterations. The RMS value with the Hybrid Method is converged after 20 iterations. This is confirmed by the DAMAS noise source map with the Hybrid Method after 100 iterations where the source position is represented by a single spot. Therefore, the proposed method is able to correctly detect and quantify a controlled monopole source in the presence of the flow.

4.4. Localization of a rod in a flow

To demonstrate the ability of the source detection algorithms, the controlled acoustic source is replaced by an aeroacoustic source. The positions of the cylinder are ($x_s=1$ m; $z_s=0.95$ m). The length of the cylinder is 0.45 m and is placed between $y_s=0.70$ m and $y_s=1.15$ m. The noise generated by vortex shedding behind a cylinder has been extensively studied [22,23]. It is known that the emitted noise is a pure tone and radiates like a dipole, the axis of which is perpendicular to the rod and to the flow. Moreover the vortex shedding frequency is related to the emitted acoustic frequency. The aerodynamic measurements show that the vortex shedding frequency is 760 Hz. Moreover the Reynolds number $Re = 10^4$ corresponds to a subcritical regime where the vortex shedding noise is strong [22]. Since the dipole is aligned in a direction perpendicular to the microphone array, the dipolar nature of the sound radiation cannot be captured. The goal is to verify that the aeroacoustic source is correctly localized. The power spectral density of all microphone signals shows a tone at 768 Hz close to the vortex shedding frequency, determined from aerodynamic measurements. Therefore, the source detection algorithms are implemented at this frequency.

The beamforming noise source map is shown in Fig. 9a. A main large spot is apparent at the position of the rod, but strong side lobes prevent the actual detection of the source position. The beamforming noise source map confirms that the sound level radiated by the interaction of the flow with the rod is low in relation to the background noise of the wind-tunnel. Fig. 9c shows the Clean-SC noise source map. In this case, the loop factor is set to 0.1 to increase the number of iterations. The noise source map obtained exhibits a main spot at the rod position, with side lobes partially removed. The Hybrid Method noise source map (Fig. 9b) further reduces the level of side lobes and exhibits a main lobe at source position. The source levels estimated by the three microphone array techniques are similar. With DAMAS, the best result is obtained with the Hybrid Method (Fig. 9e), for which the noise source map shows a single spot at the source position. While DAMAS with beamforming did not converge after 500 iterations the Hybrid Method allows DAMAS to converge after only 60 iterations.

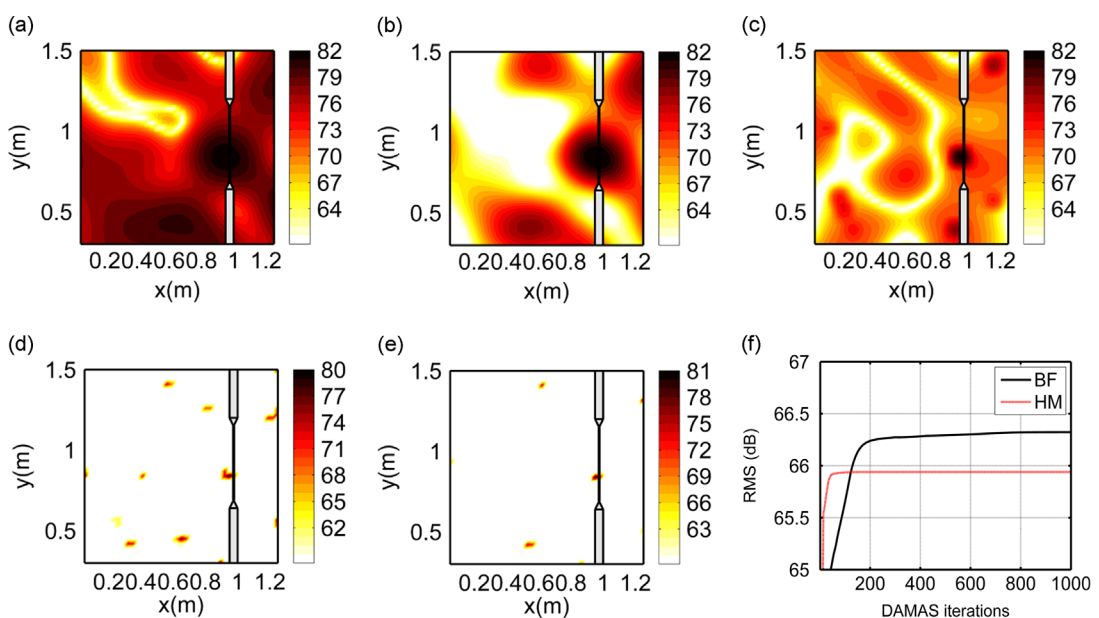


Fig. 9. Noise source maps with a rod immersed in a flow ($U_0 = 23$ m/s). (a) Beamforming, (b) Hybrid Method, (c) Clean-SC, (d) DAMAS (BF) after 100 iterations, (e) DAMAS (HM) after 100 iterations and (f) Root Mean Square of the noise source maps versus the number of DAMAS iterations. The source level is in dB and one color level represents 1 dB. (For interpretation of the references to color in this figure caption, the reader is referred to the web version of this article.)

5. Conclusion

In this paper, several source localization methods, especially for aeroacoustic problems, have been presented. The Hybrid Method which is based on an inverse problem with beamforming regularization and a data scaling has been introduced. In comparison with Gauthier et al. [10], where inverse problem with beamforming regularization matrix was introduced for the purpose of sound field extrapolation, a novelty of this paper was the introduction of this data scaling in order to fulfill the needs of acoustical imaging application. To validate the microphone array techniques, noise source maps for a simulated monopole have been compared. The Hybrid Method improves the noise source map in terms of resolution and recovers the source strength. Using DAMAS with the Hybrid Method as the initial step clearly improves the results by decreasing the number of DAMAS iterations. Next, an experiment has been carried out in a closed loop wind-tunnel. Two kinds of sources have been used, a controlled acoustic monopole driven by a sine-wave and an aeroacoustic source which is a rod immersed in a flow. In the absence of flow, the different microphone array techniques detect the source position, therefore the hard wall reflections of the wind-tunnel test section do not prevent source identification in this case. When flow is introduced, we use the convected Green function to take into account the flow effect. The convected Green function corrects the source position shift due to the flow and leads to correct source localization with all the algorithms. In the case of the rod immersed in the flow, beamforming gives a poorly resolved noise source map. The Hybrid Method and Clean-SC improve the noise source map by removing the side lobes and narrowing the main lobe. Combined with DAMAS, the Hybrid Method gives the best noise source map and clearly decreases the number of iterations. Overall, the results demonstrate the potential of the approach to localize aeroacoustic sources.

References

- [1] U. Michel, History of acoustic beamforming, *1st Berlin Beamforming Conference (BEBEC)*, Berlin, 2006.
- [2] T.J. Mueller, *Aeroacoustic Measurements*, Springer, Berlin, 2002.
- [3] T.F. Brooks, W.M. Humphreys, A deconvolution approach for the mapping of acoustic sources (DAMAS) determined from phased microphone arrays, *Journal of Sound and Vibration* 294 (4–5) (2006) 856–879.
- [4] R.P. Dougherty, Extension of DAMAS and benefits and limitations of deconvolution in beamforming, *11th AIAA/CEAS Aeroacoustics Conference (26th AIAA Aeroacoustics Conference)*, AIAA 2005-2961, 23–25 May, Monterey, CA, 2005.
- [5] T.F. Brooks, W.M. Humphreys, Extension of DAMAS phased array processing for spatial coherence determination (DAMAS-C), *12th AIAA/CEAS Aeroacoustics Conference (27th AIAA Aeroacoustics Conference)*, AIAA 2006-2654, 8–10 May, Cambridge, MA, 2006.
- [6] P. Sijtsma, Clean based on spatial source coherence, *International Journal of Aeroacoustic* 6 (4) (2007) 357–374.
- [7] T. Suzuki, L1 generalized inverse beam-forming algorithm resolving coherent/incoherent, distributed and multipole sources, *Journal of Sound and Vibration* 330 (4) (2011) 5835–5851.
- [8] T. Yardibi, J. Li, P. Stoica, L.N. Cattafesta, Sparsity constrained deconvolution approaches for acoustic source mapping, *Journal of the Acoustical Society of America* 123 (5) (2008) 2631–2642.
- [9] N. Chu, A. Mohammad-Djafari, J. Picheral, Robust Bayesian super-resolution approach via sparsity enforcing a priori for near-field aeroacoustic source imaging, *Journal of Sound and Vibration* 332 (2013) 4369–4389.
- [10] P.A. Gauthier, C. Camier, Y. Pasco, A. Berry, E. Chambatte, R. Lapointe, M.A. Delalay, Beamforming regularization matrix and inverse problems applied to sound field measurement and extrapolation using microphone array, *Journal of Sound and Vibration* 330 (24) (2011) 5852–5877.
- [11] C. Hansen, *Rank-Deficient and Discrete Ill-Posed Problems: Numerical Aspects of Linear Inversion*, SIAM, Philadelphia, 1998.
- [12] A. Moorhouse, Compensation for discarded singular values in vibro-acoustic inverse methods, *Journal of Sound and Vibration* 267 (2003) 245–252.
- [13] Y. Kim, P.A. Nelson, Optimal regularisation for acoustic source reconstruction by inverse methods, *Journal of Sound and Vibration* 275 (3–5) (2004) 463–487.
- [14] H.G. Choi, A.N. Thite, D.J. Thompson, Comparison of methods for parameter selection in Tikhonov regularization with application to inverse force determination, *Journal of Sound and Vibration* 304 (3–5) (2007) 894–917.
- [15] Q. Leclerc, Acoustic imaging using under-determined inverse approaches: frequency limitations and optimal regularization, *Journal of Sound and Vibration* 321 (3–5) (2009) 605–619.
- [16] P.A. Nelson, A review of some inverse problems in acoustics, *International Journal of Acoustics and Vibration* 6 (3) (2001) 118–134.
- [17] P.A. Nelson, S.H. Yoon, Estimation of acoustic source strength by inverse methods. Part I. Conditioning of the inverse problem, *Journal of Sound and Vibration* 233 (4) (2000) 643–668.
- [18] G.H. Golub, C.F.V. Loan, *Matrix Computations*, John Hopkins University Press, Baltimore, 1996.
- [19] C. Hansen, The discrete Picard condition for discrete ill-posed problems, *BIT Numerical Mathematics* 30 (4) (1990) 658–672.
- [20] V. Fleury, L. Coste, R. Davy, A. Mignosi, J.M. Prosper, C. Cariou, Optimization of microphone array wall-mountings in closed-section wind tunnels, *16th AIAA/CEAS Aeroacoustics Conference*, AIAA 2010-3738, 7–9 June, Stockholm, Sweden, 2010.
- [21] O. Robin, A. Berry, S. Moreau, S. Campeau, Experimental reproduction of random pressure fields for vibroacoustic testing of plane panels, *19th AIAA/CEAS Aeroacoustics Conference (34th AIAA Aeroacoustics Conference)*, 27–29 May, Berlin, Germany, 2013.
- [22] R.H. Schlinker, M.R. Fink, R.K. Amiet, Vortex noise from nonrotating cylinders and airfoils, *AIAA Paper*, vol. 38, 1976, pp. 76–81.
- [23] F.V. Hutcheson, T.F. Brooks, Noise radiation from single and multiple rod configurations, *International Journal of Aeroacoustic* 11 (3–4) (2012) 291–334.
- [24] T. Padois, C. Prax, V. Valeau, Numerical validation of shear flow corrections for beamforming acoustic source localisation in open wind-tunnels, *Applied Acoustics* 74 (4) (2013) 591–601.